CHAPTER 13

New Approaches Towards the Design of Tough Amphiphilic Polymeric Co-networks

Shereen Tan,[a] Nicholas Jun-An Chan, [a] Joe Collins, [a] Qiang Fu, [a] Greg. G. Qiao [a,*]

[a]Polymer Science Group, Department of Chemical and Biomedical Engineering, The University of Melbourne, Parkville, VIC 3010, Australia

*Corresponding contributor. E-mail: gregghq@unimelb.edu.au

Abstract

The application of hydrogel networks has long been used in industry since the 1960s. However, conventional polymeric hydrogels have limited application due to their inherent mechanical weakness. This is attributed to irregular cross-linking density, high proportion of dead, non-load bearing (elastically inactive) chains, and irregular distance between cross-linking points. In recent years, ground-breaking studies focusing on the development of novel approaches to fabricate near-ideal polymeric hydrogel networks with excellent mechanical properties have been developed. In this review Chapter, these new approaches will be outlined, with specific interest in amphiphilic polymeric co-networks, *i.e.*, networks containing both hydrophilic and hydrophobic domains. The ability to generate these near-ideal networks, which often also possess "smart" stimuli-responsive properties, would allow (amphiphilic) polymeric co-networks to be used in a wide range of advanced applications, including soft robotics, biomaterials and materials science. These new synthesis methodologies will be described in this review and will be separated into either fundamentally altering the network architecture, and/or by employing facile and orthogonal coupling chemistries.

13.1 Introduction

Polymeric hydrogels represent a class of "soft matter" which can be defined as three-dimensional cross-linked (either covalently or physically) networks capable of retaining significant amounts of water (over 90% water by mass) without flow.[1, 2] Owing to their soft and rubbery consistence, they are often regarded as being similar to the extracellular matrix (ECM) of biological tissue. Although initially developed in the 1960s for use as soft contact lenses to treat myopia,[1, 3] in the past decade, interest (in both academia and industry) to further develop polymeric hydrogels for other applications has exploded due to the compositional flexibility and high tailorability synthetic polymer chemistry provides.[4] This notion can be observed by the widespread use and continued exploration of polymeric hydrogels in many broad and far-reaching fields, including engineering (*e.g.*, soft robotics,[5, 6] wearable electronics[7, 8]), biotechnology (*e.g.*, tissue engineering,[1, 9, 10] drug delivery[9, 11]) and materials science (*e.g.*, elastomeric materials,[12-14] purification and separation[15, 16]). However, the use of polymeric hydrogels in these fields is compromised by their inherent mechanical weakness. Conventional polymeric hydrogel networks, synthesised by free radical polymerisation, are particularly known to display poor mechanical properties. These undesirable characteristics are attributed to (i) the high dispersity in the molecular weights of the elastically active chains, (ii) the inhomogeneity at the cross-linking nodes, and (iii) the presence of a high proportion of dangling, non-load bearing chains,[17, 18] all three of which arise from the lack of control inherent in free radical polymerization systems. These characteristics result in networks which are far from ideal. For example, although swollen hydrogels are generally soft, they often suffer from pre-mature fracture (due to uneven load distribution throughout the hydrogel network), and also exhibit extremely slow responsiveness, both of which are undesirable properties limiting

their real-word applications.[19] Thus, improving the mechanical performance of conventional polymeric hydrogels represents a very timely challenge.

In recent years, researchers have been addressing this challenge by developing innovative concepts which would allow polymeric networks to not only acquire superior mechanical properties with customisable stimuli-responsiveness (*e.g.*, temperature, pH, oxidation), but also to acquire the ability to "react" rapidly to changes in the external environment.[17, 20-22] In light of such ground-breaking studies, this Chapter will focus on new emerging approaches which could result in the fabrication of ideal networks with extreme toughness based on fundamentally altering the network architecture and/or by employing facile coupling chemistries (Figure 13.1). Each individual method will be fundamentally outlined, with specific interest in amphiphilic polymeric co-networks (APCN), that is, networks containing both hydrophilic and hydrophobic domains. The formed APCNs often also possess stimuli-responsiveness ("smart" behaviour) enabling their use in advanced applications.

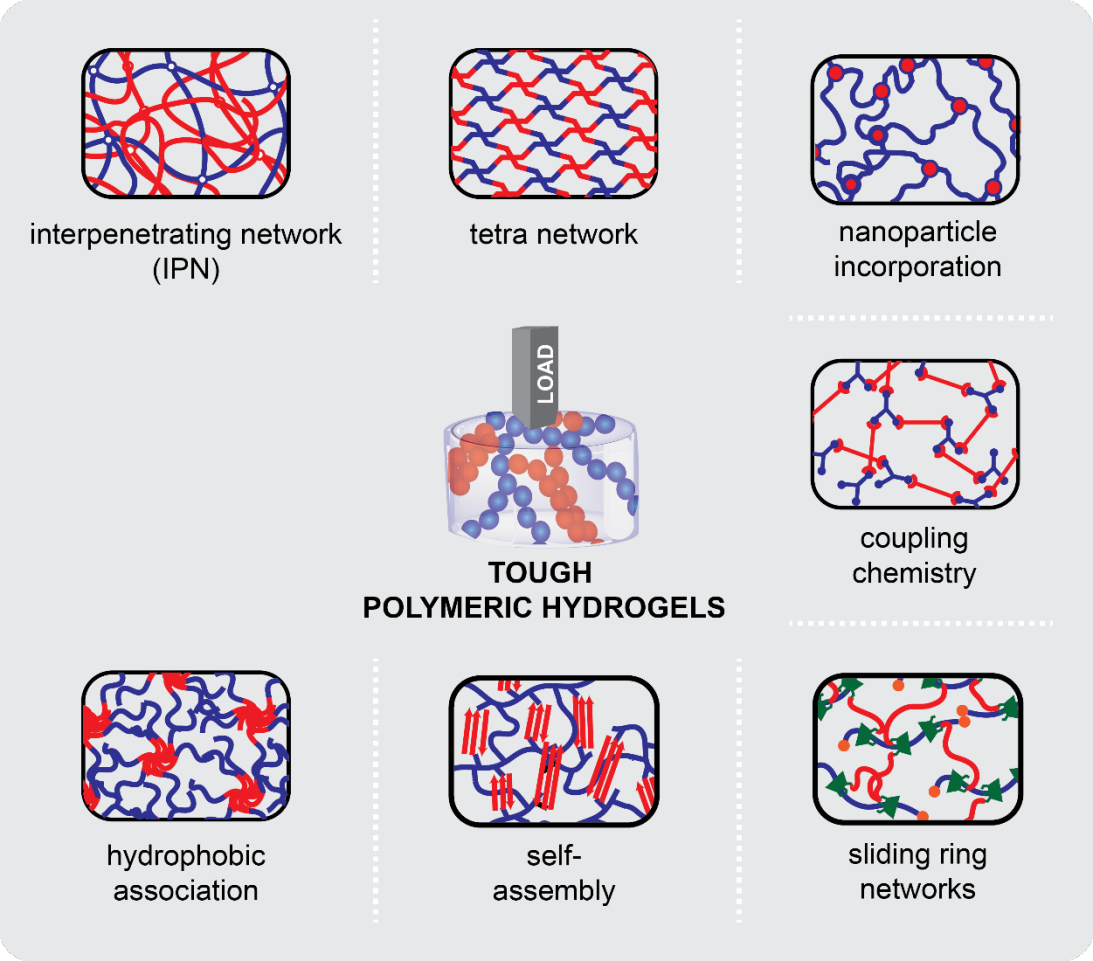

Figure 13.1. Graphical illustration of the new approaches used to fabricate tough polymeric hydrogel networks.

It should be noted that, in this chapter, the term "toughness" is used to describe the ability of a material to absorb mechanical energy, *i.e.*, in J m^{-3} units, and deform without fracturing, while "stiffness" is the Young's modulus of the material, *i.e.*, the ratio of stress to strain in the linear deformation region, with units of Pascal (Pa). Note that this review will highlight only recent literature examples as significant advances in materials science have developed in the last decade. For an overview of this field covering the late 1990s to early 2000s, readers are referred to the literature authored by Patrickios *et al.*,[23, 24] and Gong *et al.*[20]

13.2 Mechanical Properties of Hydrogel Networks

The mechanical properties of hydrogel networks are largely determined by the cross-linking density and overall rigidity of the polymer chains.[25] Although increasing the overall polymer concentration and/or increasing the cross-linking density can improve the overall hydrogel stiffness, the formed hydrogels often still suffer from low toughness, elasticity, and strength recoverability. These traits are often necessary for real-world applications, specifically for repeated load bearing environments. Furthermore, while increasing the polymer concentration may improve the mechanical properties of the hydrogel, this inevitably leads to a decrease in the hydrogel water content, thereby affecting swellability. High water content and swellability are vital properties required for tissue engineering applications, as hydrogels with high water content often resemble the ECM of biological tissues.[9, 25]

Traditionally, the poor mechanical performance of hydrogels can be attributed to their inherent structural inhomogeneity which arises from (i) an irregular distribution of cross-linking points throughout the network, (ii) widely-differing polymer chain lengths between cross-linking points, and (iii) high water content. Regarding the first aforementioned factor, densely cross-linked regions initially form, which are subsequently linked by longer polymer chains. Thus, when stress is applied to the hydrogel, the force is not evenly distributed across the entire network and the cross-linking points separated by the shortest polymer chains break first, resulting in localised fractures which continuously grow. Regarding the second factor, if a cross-linking agent is employed, it is often difficult to ensure that cross-linking will occur at regularly spaced intervals, which again results in network inhomogeneity. Finally, when dried hydrogels are submerged in aqueous media, they are able to absorb an amount of water more than 10 times their original dry mass. During swelling, the polymer chains separate, which results in a significant reduction in the energy dissipation efficiency and significantly reduces the toughness of the hydrogel.

13.3 Coupling Chemistry

In trying to overcome the irregular cross-linking density, significant research has been made to find new methods to prepare tougher hydrogel structures. The use of rapid coupling chemistries (Figure 13.1a), including acid-chloride reactions, has been explored to fabricate amphiphilic hydrogel films.[26] Although, film formation is evident, the sensitivity of the reaction towards water, and the rapid uncontrollable kinetics often result in network inhomogeneity due to unevenly distributed cross-linking densities and/or incomplete reactions. In overcoming these drawbacks, one valid methodology involves the exploitation of efficient, robust and highly orthogonal coupling chemistries.

The very high efficiency of click reactions[27] (*e.g.*, thiol-ene, azide-alkyne, thiol-yne, Diels-Alder, and carbonyl condensations) allows for the creation of nearly ideal hydrogel networks with significantly improved mechanical properties compared to traditional free radical chemical cross-linking (Figure 13.2).[28, 29] Additionally, the selectivity/ bio-orthogonal nature of click reactions, as well as the absence of toxic by-products, make click chemistry an attractive candidate for biomedical applications. It was reported by Malkoch *et al*. that only 0.2% of functional groups within a hydrogel remained unreacted following the copper-catalysed azide-alkyne cycloaddition (CuAAC) click reaction.[28] The very high efficiency of the CuAAC is expected to result in a more even distribution of cross-linking points, forming a near-ideal structure with much improved physical properties. Undoubtedly, the CuAAC click reaction is the most popular click reaction to date, due to the very high coupling efficiency. However, the CuAAC requires a copper metal catalyst which must be removed from the final product, if the end application is biological.

[Figure 13.2 near here]

Figure 13.2. Preparation of hydrogels using highly efficient click chemistry. Common click reactions, for example the CuAAC, Diels-Alder, and thiol-ene reactions are shown as well as some of the advantages of click hydrogels over conventional free radical or photo-chemically cross-linked hydrogels.

While many hydrogels have been prepared using a variety of click reactions, most reports involve the preparation of purely hydrophilic materials.[30-34] The development of amphiphilic materials offers several advantages, and thus has recently become more popular. This includes the incorporation of natural,[35] synthetic and amphiphilic polymers.[29] One example is the preparation of APCNs prepared *via* click chemistry based on modified elastin-like proteins (ELP).[35] ELPs consist of an elastomeric central block with self-assembling, hydrophobic end-blocks. The self-assembly of ELPs creates physical cross-links which can be reinforced by chemical cross-linking, thereby vastly improving the materials mechanical properties. By modifying glutamic acid residues in the ELP backbone with aldehyde or hydrazide functionality, effective crosslinking through hydrazone formation could be achieved. The ultimate tensile strength of the ELP hydrogels ranged from 0.49 – 4.12 MPa, which is in the range of soft tissues such as blood vessel walls (0.4 – 2.0 MPa) and the human urinary bladder (~0.27 MPa).[35]

A tough APCNbased on polyurethane and poly(ethylene glycol) (PEG) was recently prepared using CuAAC.[29] By using monomers of an exact size and highly efficient CuAAC coupling, hydrogels exhibiting excellent mechanical properties were prepared. Under compression, the hydrogels could sustain stresses between 2.16 and 43.05 MPa (deformation ratios between 44.1 and 82.6%). Further, when stretched, the hydrogels could sustain stresses between 0.53 and 2.04 MPa (deformation ratios between 223 and 658%). Finally, the hydrogels exhibited low/no

toxicity to human lung fibroblastic cells (WI-38), with high cell viability and no changes to cell morphology after 3 days of incubation.[29]

While the CuAAC reaction was used to prepare biocompatible materials, there is still risk that trace amounts of Cu remaining within the hydrogel matrix will have adverse effects on health. In light of this, the copper-free strain-promoted alkyne-azide cycloaddition (SPAAC) was developed.[36-38] SPAAC was used to prepare a wide range of biocompatible hydrogels based on hydrophilic polymers such as hyaluronic acid/PEG,[39] PEG,[40-44] and PEG/polypeptide.[45] Again, however, there remain only a limited number of examples of amphiphilic hydrogels prepared using the SPAAC click reaction. This may be attributed to solvent incompatibility.

One such amphiphilic hydrogel was reported by Ono *et al.*[46] This hydrogel was prepared using SPAAC to cross-link micelles with amphiphilic triblock copolymers.[46] The azide and cyclooctyne-functional triblock copolymers were prepared by ring-opening polymerisation (ROP) of a cyclic carbonate using PEG as a macro-initiator. Gelation occurred rapidly (< 60 s) upon mixing the two monomers without the need for a Cu catalyst. FTIR analysis revealed the complete disappearance of the azide peak indicating very high conversion. The addition of micelles to the hydrogel was found to decrease the storage moduli, in a particular case from 323 down to 161 Pa. Importantly, the DOX-loaded micelle/hydrogel complexes displayed shear-thinning behaviour and were, therefore, able to be injected through a 22G syringe needle. Finally, the hydrogels were shown to gradually release DOX over 1 week and to be active against human breast cancer (MDA-MB-231) cells (28% cell survival after 48 h) indicating their potential application as injectable therapeutics.[46]

As well as the SPAAC reaction, other click reactions that do not require toxic catalysts, such as the Michael addition[47] and the Diel-Alder reaction,[48] have been used to prepare tough hydrogels. Wooley and co-workers used the Diels-Alder click reaction to prepare amphiphilic polymer co-networks for use as self-healing, anti-biofouling surfaces.[48] These co-networks were composed of furan-functionalized fluoropolymers and maleimide-functionalized PEG. Protein absorption on the amphiphilic surfaces, as investigated using atomic force microscopy, was found low but indicated a topographically complex and rough surface.

13.4 Interpenetrating Networks (IPN)

Aside from utilising efficient, orthogonal coupling chemistries, the overall network architecture can also be tuned to generate mechanically tough hydrogel networks. This includes interpenetrating networks (IPN) (Figure 13.1b). The term IPN was coined in 1977,[49] and describes hydrogels formed from two or more polymer networks that are not covalently linked, and where at least one of the networks is formed in the presence of the other(s) (Figure 13.3a). The resulting interpenetration of the individual networks allows the materials to absorb significantly larger amounts of mechanical energy without fracturing,[20] when compared to the corresponding single network hydrogels. The need for tougher hydrogel materials arose because traditional elastomeric (non-hydrated polymer) networks are often plagued with severe brittleness, especially at low temperatures, and plasticisation at high temperatures due to high chain mobility. Although researchers could develop IPNs in 1914, aspects regarding phase separation and morphology were not well understood.[49, 50] Based on current understanding, many IPNs show dual phase continuity, where two or more polymers in the system form a continuous phase at the macroscopic scale. Therefore, interpenetration of the two networks does not occur on a molecular scale, but, instead, discrete phases of interpenetration at scales

of only tens of nanometres are present.[49, 50] There are two main synthetic procedures towards the fabrication of IPN; by simultaneously mixing the respective monomers and subsequently inducing polymerization, or by sequential polymer cross-linking. In sequential polymer cross-linking, the second monomer is reacted within the initial polymer network to form the second IPN.

13.4.1 Double Network (DN) Hydrogels

In 2003, Gong and co-workers made a breakthrough in the development of IPN networks, where double networks (DN) hydrogels were fabricated for the first time, and found to have extreme toughness while maintaining a very high water content (90% w/w of water).[51] In this work, a two-step sequential cross-linking method was utilised to prepare the DN hydrogel. First, a densely cross-linked hydrophilic network consisting of poly(2-acrylamindo-2-methylpropanesulfonic acid) (PAMPS) and *N,N′*-methylenebisacryalmide (MBA) was prepared utilising free radical photopolymerisation (Figure 13.3a).[51] The PAMPS network was subsequently swollen in an aqueous solution of acrylamide (AAm), MBA and a radical photoinitiator. Photopolymerisation of the AAm resulted in the formation of the second network, thereby yielding the final IPN. In this important first work, the authors found that the DN hydrogel could resist cutting with a slicer (Figure 13.3b), exhibiting high compressive fracture strength (17.2 MPa) and strain (λ = 82%). Such mechanically robust hydrogels could be formed when the following considerations are satisfied; (i) the first network is highly cross-linked while the second network is loosely cross-linked, and (ii) the ratio of the polymer volume fractions of the second network to the first network is about ten. Given that the compressive stress-strain curve of the DN gel overlaps with that of the PAMPS single network gel at low strains (up to 20%), it could be concluded that the first network mainly contributes

to increasing the stiffness of the DN gel; furthermore, because the DN gel has a similar (and slightly higher) compressive fracture strain to that of the second network, it could be inferred that the second network mainly contributes to increasing the strain (ultimate deformability) of the DN gel (Figure 13.3c).[51] The mechanism behind obtaining such mechanically tough networks is attributed to the presence of sufficient fluidity (*i.e.*, viscosity) within the second network to effectively dissipate mechanical energy and stress, and prevent crack propagation within the first network, a hypothesis supported by the loose cross-linking in the second network. Additionally, the method outlined was found to be highly versatile and could be applied towards natural biocompatible polymers, including collagen, agarose, and bacterial cellulose, allowing for tough DN hydrogels to be used not only in industrial applications but also in biotechnology and tissue engineering.

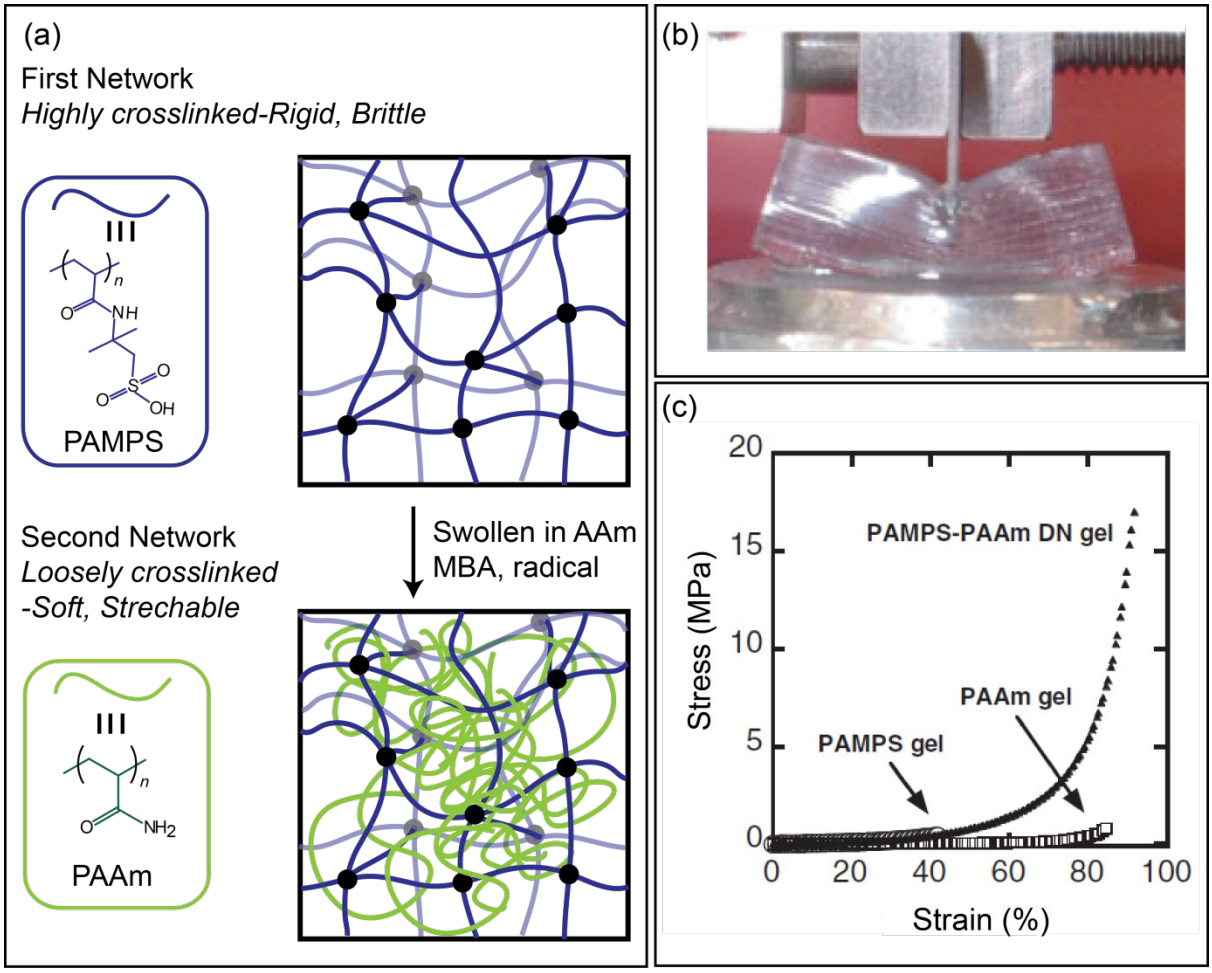

Figure 13.3. (a) Graphical illustration of ultra-tough DN hydrogels through the sequential free radical photopolymerisation of AMPS followed by AAm. (b) Photograph of the formed DN hydrogels demonstrating resistance to slicing. (c) Compressive stress-strain curve of the DN hydrogel versus those of the individual single networks composed of PAMPS and PAAm. Images adapted with permission from ref 51.

Although this work allowed for the generation of tough hydrogel networks whilst maintaining high water swellability, the ability to undergo repeated cycles of loading was limited. This is because the high toughness of the DN hydrogels is also accompanied by irreversible fracture of the covalent bonds in the first, brittle network, which helps dissipate a significant amount of mechanical energy onto the overall network. This permanent breakage limits the

application of DN hydrogels for repeated load bearing applications often required in industry. Methods which have been commonly used to circumvent this issue include the introduction of (i) ionic interactions,[52-56] (ii) dynamic bonds,[57, 58] (iii) crystalline domains[59, 60] and/or (iv) hydrophobic components[58, 61, 62] all of which can assist in energy dissipation. Although ionic bonds have been incorporated into DNs, the instability of these interactions in saline conditions limits their application in some physiological environments. The introduction of dynamic bonds allows IPNs to withstand repeated loading-unloading cycles due to the reversibility of the bonds, whilst also allowing the networks to be extruded through fine orifices, including syringes which can be of particular importance in tissue engineering and drug delivery applications.[57]

Of particular interest to this review, Gong and co-workers recently developed physical amphiphilic DN hydrogels which are tough, stiff and recoverable. Specifically, the first network was formed through the hydrophobic association of the amphiphilic triblock copolymer, poly(*n*-butyl methacrylate)-*b*-poly(methyacrylic acid)-*b*-poly(*n*-butyl methacrylate) (PBMA-*b*-PMAA-*b*-PBMA), with a M_w of 60 800 Da (Figure 13.4a).[62] Self-assembly was induced by first dissolving the polymer in *N*,*N*-dimethylformamide (DMF), subsequently pouring the resulting solution into a rectangular mould, and, finally, spraying water vapour onto the surface, which triggered the aggregation of the hydrophobic domains, resulting in block copolymer self-assembly and physical gelation (Figure 13.4a).[62] It should be noted that the central hydrophilic block in this copolymer is flanked by hydrophobic blocks. The block copolymer physical hydrogel was subsequently immersed in an AAm monomer solution containing a photoinitiator, and was subjected to UV irradiation, resulting in the formation of linear PAAm chains. Physical cross-linking between the first and second networks was then achieved through hydrogen bonding between the pendant amide groups of

PAAm (second network) and the carboxylic acid groups of the middle hydrophilic block of PBMA-*b*-PMAA-*b*-PBMA (first network) (Figure 13.4a).[62] DN gels synthesised using a 3 M concentration of AAm were deemed optimal, and wereas the ones examined in the work described later herein. Small angle X-ray scattering (SAXS) analysis was conducted to elucidate the morphology of the networks. This analysis indicated that the first network consisted of randomly distributed spherical hydrophobic domains acting as the cross-linking sites.[62] Upon incorporation of the second network, a slight decrease between the distances of the hydrophobic domains was observed, which was attributed to the formation of hydrogen bonds between the first and second network, and confirmed *via* Fourier transform infra-red spectroscopy (FT-IR).[62] By deriving values obtained from the Arrhenius plot, the authors noticed two apparent activation energy values (E_a) of ~254 and ~180 kJ mol^{-1}, with relaxation times of ~ 4.1 × 10^4 s and ~ 5 × 10^{-2} s, which corresponded to the hydrophobic associations and the hydrogen bonds, respectively.[62] Thus, it is clear that, within this network, the hydrophobic associations, which are strong and exhibit long relaxation times, act as permanent cross-links, while the hydrogen bonds, which are week and exhibit short relaxation times, act as sacrificial bonds in the gel. The mechanical performance of the DN gels was characterised and compared to gels made of the individual components of the first networks (SN) in terms of uniaxial tensile stress and pure shear tests. Uniaxial compressive tests revealed that the DN gel was *ca.* 43 times stiffer than the SN, with respective Young's moduli of 2.2 ± 0.2 MPa and 0.051 ± 0.04 MPa, and was 55 times stronger than the SN, with respective fracture stresses of 10.5 ± 1.4 MPa and 0.19 ± 0.04 MPa. Interestingly, unlike other DN gels which observe yielding or strain softening, the DN gels in this report showed a linear stress-strain curve up to a 600% strain (Figure 13.4b).[62] Figure 13.4e shows the self-recovery properties of these DN gels *via* cyclic tensile loading-unloading tests for different waiting

times. At room temperature, a large hysteresis was observed, indicating that there was bond rupture during stretching, which dissipated energy. Except for the first cycle, a quick recovery with an efficiency of 85% could also be observed.[62] As both types of bonds were physical, reformation of the ruptured interactions was possible and was achieved by performing a heating (1 min)-cooling (15 min) process (Figure 13.4e).[62] In showing their mechanical robustness, the DN gels could withstand a 1 kg weight without rupture, and the gel could be tied into a knot, subjected to stress, and, upon release, it could reform into its original form (Figure 13.4c-d). Self-healing between two cut surfaces of the gels could also be achieved as the bonds are physical. Briefly, this was conducted by (i) immersing the cut edges in DMF, a good solvent, which gives chain mobility, (ii) subsequently bringing into contact the edges and heating at 60 °C for 60 min, and, finally (iii) immersing the joined gel in water to extract any remaining DMF.[62] Figure 13.4f shows images of the healed DN gel. As not all the defects could be healed, a drawback commonly observed in these types of networks, the original tensile fracture stress of the gels of ~10 MPa could not be retained, with the healed DN gel displaying a fracture stress of only 2.3 MPa (Figure 13.4g). Although lower than that of the original (virgin) gel, this fracture stress was the highest thus-far value reported for healed gels.

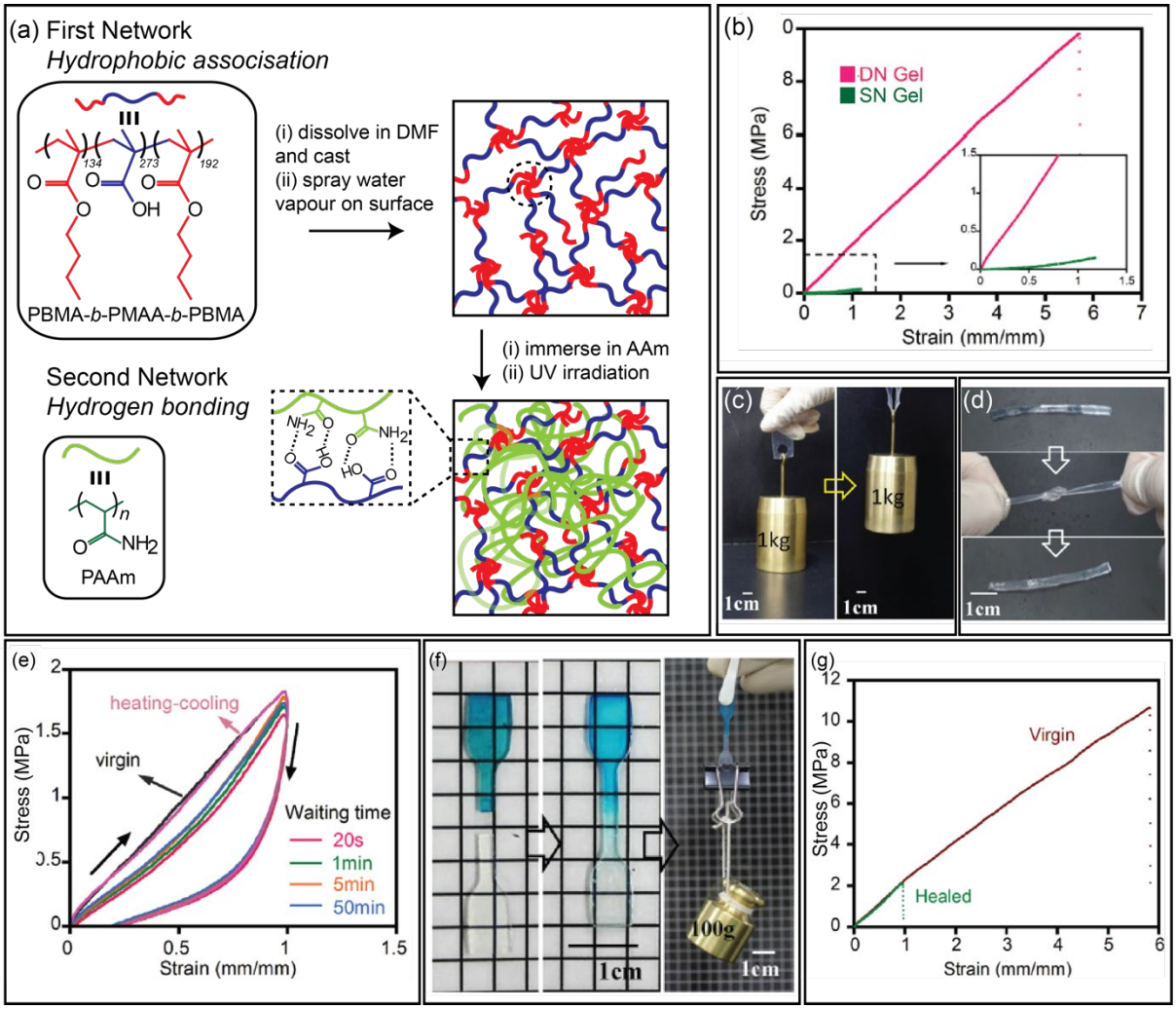

[Figure 13.4 near here]

Figure 13.4. (a) Graphical illustration of the DN hydrogels prepared through the hydrophobic association of the PBMA-*b*-PMAA-*b*-PBMA amphiphilic triblock copolymer, and subsequent hydrogen bonding between the carboxylic acid groups of the first physical network and the amide groups of the second network. (b) Tensile stress-strain curves for the prepared DN and SN hydrogels. (c-d) Photographic images of the DN hydrogels demonstrating high strength and toughness. (e) Cyclic tensile loading-unloading tests of DN networks using different waiting times. (f) Self-recovery properties of DN hydrogels, and (g) Tensile stress-strain curves for the pristine (virgin) DN gel and the healed sample. Images adapted with permission from ref 62.

Of particular note is that amphiphilic DN hydrogels have also been fabricated using CuACC click chemistry.[63] The highly efficient coupling chemistry provides an attractive means to prepare tough hydrogels under mild, bio-orthogonal conditions, devoid of toxic or expensive catalysts. Initial network formation was achieved between azide di-functional PEG and PEG with alkyne side chains. PEG with dopamine side chains was also physically incorporated into this initial network. The second network was then formed by the addition of Fe^{3+}, which resulted in iron complexation, through the dopamine side chains. In showing increased toughness, the DN could withstand pressures up to 2.26 MPa (~2.8 times more than the PEG based initial network).[63] Additionally, the IPN hydrogels were found to elicit no inflammatory response when implanted into pigs, thereby demonstrating good biocompatibility. Finally, the IPNs were found to slowly degrade under physiologically relevant conditions (0.01 M PBS at 37 °C), degrading to 47.3% of their initial weight after 8 weeks.

Of further interest, other groups have developed more sophisticated macromolecules which could be incorporated into the DN architecture. This involved the inclusion of amphiphilic star copolymers.[64, 65] The general idea behind this concept is that the amphiphilicity of the first network will drive phase separation on the nanoscale, resulting in hydrophobic nano-domains, which can provide another mechanism for energy dissipation. The Patrickios group has widely explored this area where star block copolymers have been synthesised and cross-linked together to form the first network.[64, 65] The second network is introduced by using conventional free radical polymerisation. In one example, the star polymers were made *via* a five-step, sequential, one-pot procedure using group transfer polymerisation (GTP).[65] The hydrophilic monomer, 2-(dimethylamino)ethyl methacrylate (DMEAMA) was first polymerised using the initiator 1-methoxy-1-trimethylsiloxy-2-methyl propene (MTS) to synthesise the linear hydrophilic homopolymers which would subsequently constitute the

arms of the star. These arms could then be cross-linked using ethylene glycol dimethacrylate (EGDMA) to generate hydrophilic "arm-first" star homopolymers. Upon subsequent addition of DMEAMA, "in-out" star homopolymers were synthesised. Amphiphilic star block copolymers could then be obtained by the addition of lauryl methyacrylte (LauMA). A subsequent second addition of EGDMA led to the formation of the final amphiphilic polymer co-network (APCN), which would serve as the first network for the preparation of the DN, (Figure 13.5).[65] Gel permeation chromatography-static light scattering (GPC-SLS) was conducted and revealed that the star precursors contained 7-281 arms per cross-linking node. It is noteworthy that the dangling polyDMAEMA chains were necessary to give the first network sufficient swellability in the aqueous media (the swelling was further enhanced by acidification of the first network), a feature necessary for facilitating the introduction of a large volume of the AAm and MBAAm aqueous solution, necessary for the formation of the second interpenetrating network at a high polymer volume fraction. The second networks were prepared by photo-polymerisation of AAm at a concentration of either 2 or 5 M. The mechanical properties of all the swollen networks could be characterised by bulk compression measurements. The results revealed that the strain at break for the DNs were ~80%, higher than those of the parent APCN first networks of ~60%. However, more significant was the enhancement in the stress at break which rose to 6.6-8.4 MPa, 16.5 times greater than that of the APCN single networks and 60 times greater than that of PAAm single networks.[65]

[Figure 13.5 near here]

Figure 13.5. Graphical illustration of the synthesis of amphiphilic polymer co-networks, which would subsequently constitute the first network within the final double-network.

Controlled radical polymerisation in the form of reversible addition-fragmentation chain-transfer polymerisation (RAFT) has also been used to prepare star polymers with narrow molecular weight dispersity. When incorporated into a DN network, more controlled and uniform nanophase self-assembly was observed.[64, 66] The strongest star polymer-based DN hydrogel possessed a stress at break of 3.29 MPa and a strain at break of 78% with hydrophobic domains regularly dispersed (every 15-26 nm) throughout the network.[64]

It should be noted that the simple incorporation of star polymers into hydrogels to increase their mechanical characteristics is separately described in later parts of this Chapter.

13.5 Tetra Networks

Aside from incorporating sacrificial networks which can help increase hydrogel toughness, the overall distribution of cross-linking points throughout the hydrogel network can also be finely tuned to generate homogeneous single network hydrogels (Figure 13.1c). In these hydrogels, the distance between cross-linking points is the same throughout the entirety of the network. This is achieved by the use, and subsequent cross-end-coupling, of two symmetrical, four-arm star homopolymer modules where both entities are (i) of the same size and (ii) have mutually reactive end-functional groups (Figure 13.6). Due to their homogeneous geometry, the formed networks, known as "*tetra-arm*" gels, exhibit a more uniform stress distribution (as determined by small-angle neutron scattering experiments)[67] and a more cooperative response when compared to traditional networks fabricated from conventional radical chemistry. This allows for better stress distribution over a much larger number of elastic chains.[68] In their first report, Sakai and co-workers synthesised tetra-arm gels made from tetra-amine-terminated PEG (TAPEG) and tetra(*N*-hydroxysuccinimidyl) (NHS)-glutarate-terminated PEG (TNPEG).[69] When these two polymer solutions were mixed,

amide bonds were formed between the amino groups and the succinimidyl ester groups (Figure 13.6 and Figure 13.7a).

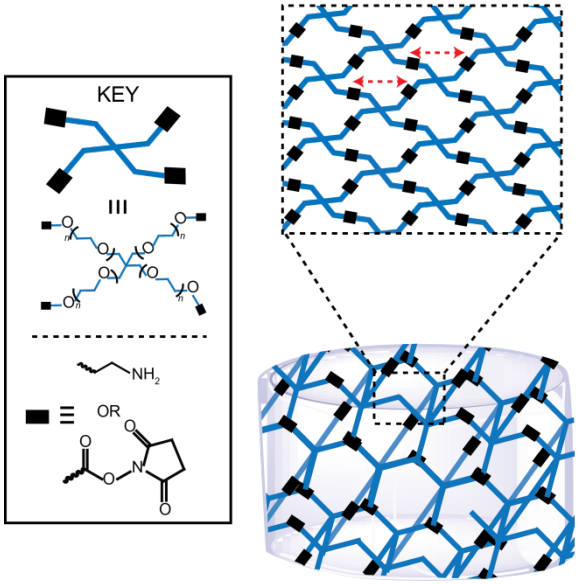

Figure 13.6. Graphical illustration depicting the molecular architecture of the ultra-tough tetra-arm gels fabricated from tetra-arm PEG derivatives.

Because conventional hydrogels equilibrium "swell" to a large extent in water, their mechanical toughness drastically weakens in aqueous media and physiological conditions. This inevitable loss in mechanical properties may limit potential applications. In trying to circumvent this issue, Sakai's research group also employed thermo-responsive hydrophobic domains to control overall swellability. Hydrophobic domains collapse above a critical temperature (T_c) due to hydrophobic interactions. This generally has been conducted using two different methods; (i) creating a hydrophilic and hydrophobic macro-cross-linker (Figure 13.7a), or (ii) utilisation of an amphiphilic macro-cross-linker (Figure 13.7b). Using the former concept, hydrophilic TNPEG with activated ester end-groups, hydrophilic TNPEG with amine end-groups and hydrophobic and thermo-responsive tetra-arm poly(ethyl glycidyl ether-*co*-

methyl glycidyl ether) with amino end-groups were homogeneously cross-linked without any organic solvent, UV irradiation or catalyst (Figure 13.7a).[70]

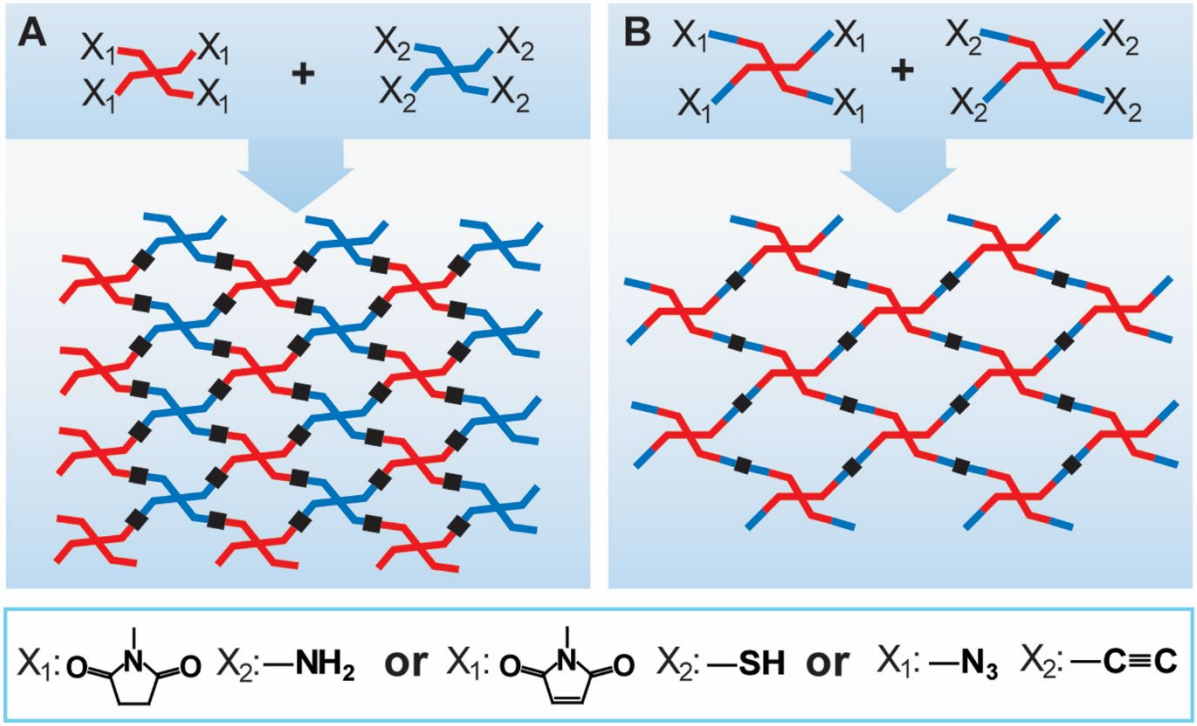

Figure 13.7. Structure of *tetra-arm* polymer network composed of: (a) same size, tetra-arm hydrophobic (red) and hydrophilic (blue) star homopolymers with reactive end-functional groups; and (b) same size, tetra-arm amphiphilic star block copolymers with reactive end-functional groups.

By tailoring the thermo-responsive segment fraction (r), the swelling ratio (Q) of the hydrogels could also be tailored, where a higher value of r expectedly resulted in a lower Q-value. When swollen at 10 °C, all of the hydrogels (r = 0.0-0.5) exhibited high Q-values (~300%) (Figure 13.8a-b).[70] However, upon increasing the temperature up to around the T_c of the thermo-responsive segment, a drastic decrease in Q could be observed. Importantly, the control over Q at a fixed T_c could not be achieved using conventional thermo-responsive hydrogels synthesised using random copolymerisation of hydrophilic and thermo-responsive monomers,

where T_c increases with an increase in the fraction of the hydrophilic monomer and can exceed 37 °C.[62] It was found that when r = 0.4, the hydrogels could retain their original volume and shape even when immersed in aqueous media at 37 °C, and still contained a high mass fraction of water, *ca.*, 90% w/w (Figure 13.8b).[70] Further, unlike their conventional analogues which develop turbidity, these hydrogels remained transparent even above the T_c. Because the mechanical properties of hydrogels are related to their water swellability, elongation tests of hydrogels containing different thermo-responsive segment fraction (r) values were conducted after the hydrogels had reached equilibrium at 37 °C (above T_c). Figure 13.8c shows representative stress-elongation curves, indicating that the maximum elongation ratio (l_{max}) was reduced with a decrease in r. In the hydrogel with r equal to 0.4, the swelling was highly suppressed, leading to enhanced mechanical properties. Specifically, the hydrogels could be stretched more than seven-fold without hysteresis, while the conventional hydrogel (r = 0) in the equilibrium state was easily torn off before the hydrogel was stretched three-fold (Figure 13.8d).[70] Overall, this study revealed the advantages of homogeneously imparting hydrophobicity throughout a hydrophilic network (hydrogel), where the (i) hydrophobic domains can serve as another cross-linking point due to their aggregation in aqueous media and (ii) the homogeneous distribution allows for transparent hydrogels, which may be of interest in optical applications.

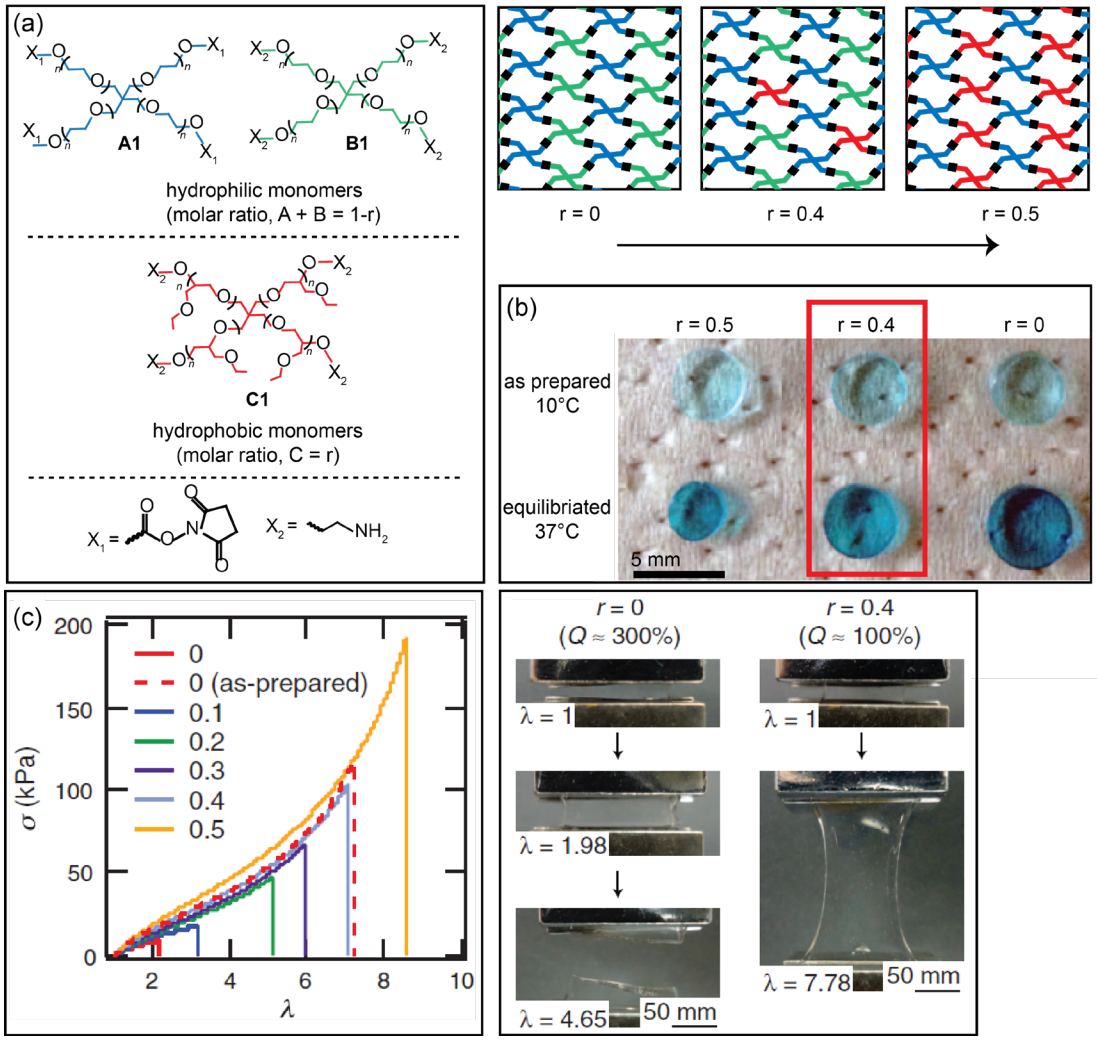

Figure 13.8. (a) Schematic illustration of the hydrogel components and graphical illustration of the network architecture with varying the thermo-responsive segment fraction *r*. (b) Photographs of the hydrogels exhibiting different swelling ratios, *Q*, in the as-prepared and equilibrium states. (c) Mechanical properties as revealed in the stress-elongation curves of hydrogels equilibrated in PBS at 37 °C. The curves are coloured according to the thermo-responsive segment fraction, *r*. (d) Photographs of hydrogels (*r* = 0.0 and 0.4) during the elongation tests. From H. Kamata, Y. Akagi, Y. Kayasuga-Kariya, U.-i. Chung and T. Sakai, Science, 2014, 343, 873-875. Reprinted with permission from AAAS.[70]

Recently, these researchers have further investigated this system and proposed a possible illustration of the network domain structure which allows this non-swelling feature. Small-angle neutron scattering (SANS) measurements indicated that, at temperatures lower than 16.6 °C, the structure of the hydrogel with $r = 0.4$ was similar to that of the purely hydrophilic hydrogel (with $r = 0$) within the same temperature range. However, at temperatures above 19.5 °C, discrete spherical domains were formed by the hydrogel with $r = 0.4$. The mean aggregation number, N_{agg}, of a single spherical domain was much higher than unity, implying that multiply aggregated thermo-responsive tetra-arm poly(ethyl glycidyl ether-*co*-methyl glycidyl ether) stars and hydrophilic tetra-arm PEG stars gathered to form a single domain. Therefore, the hydrogel ($r = 0.4$) is non-swellable because of the excess elastic energy (folding frustration) of this matrix network which cancels the osmotic pressure and induces significant macroscopic shrinking.[70]

The coupling chemistry employed to facilitate tetra-arm gel fabrication is essential as the coupling should be quantitative and each functional entity be of similar reactivity. In exploring this, Shibayama et al.[71] conducted kinetic studies on the gelation reaction of tetra-arm PEG macromolecules having amine and activated ester terminal groups using ATR-IR and UV spectroscopies. The results indicated that the reaction rate constant (k_{gel}) values for the gelation of the tetra-arm PEG gel were almost constant, within experimental error, and close to those for the linear PEG system of molecular weight of 5 kDa.[71] This trend was independent of the volume fraction and molecular weight of the macromolecules.[71] These significant results indicated that the simple chemistry used for the synthesis of the tetra-arm gels allows for homogeneous cross-linking as the diffusion of the macromolecules is much faster than the reaction rate.[71] This implies that a judicious selection of mutually reactive end-groups is necessary to obtain homogeneous gels.

Aside from the addition of hydrophobic domains,[62, 72] added complexities to conventional tetra-arm gels have also been explored.[73-76] This includes the development of a hydrogel from the pre-gel clusters based on hyperbranched oligomers of tetra-arm PEG stars.[71,73] In particular, Sakai and co-workers[73] recently reported the synthesis of a new class of hydrogel through a two-step process *via* Michael addition reactions. In the first step, the cross-linking reaction was intentionally stopped immediately prior to the gelation point. This resulted in highly branched oligo-PEG clusters with unimodal size distribution.[73] In the second step, the oligo-PEG clusters could be further co-cross-linked to form a hydrogel. Owing to the highly homogeneous aggregated clusters formed within the network, the formed hydrogel gained additional mechanical toughness, and exhibited extremely low swelling pressure which prevented severe adverse reactions in the surrounding tissue.[73]

Of particular interest to this review Chapter is the work of Oshima and Mitsukami[77] who recently reported the fabrication of amphiphilic polyelectrolyte tetra-arm gels through the synthesis of star block copolymers of sodium acrylate (NaA) and methyl acrylate (MA) (Figure 13.7b). Network formation was then accomplished *via* the CuAAC end-linking reaction. The swellability of the formed hydrogels was shown to be controlled by their macromolecular characteristics, including the overall hydrophobic content, the block sequence and way of monomer distribution (whether random or block) along the polymer chains, and the length and flexibility of the spacer between the hydrophobic segment and the main chain. The swelling ratios of the hydrogels in saline (Q_s) and pure water (Q_{pw}) were measured.[77] It was found that the Q_s and Q_{pw} ratios for the homopolymer networks of NaA and the networks consisting of amphiphilic random copolymers of NaA and MA exhibited similar values.[77] However, the swelling ratios were significantly lower for the corresponding amphiphilic block copolymer analogues. In addition, the stimuli-responsive behaviour of these block copolymer co-networks

was more pronounced towards salt as the network architecture promoted poly(methyl acrylate) association.[77] By taking advantage of the salt-responsive property of the block amphiphilic gels, the authors showed the formed networks could capture and release hydrophobic cargo in response to external salt concentration.[77]

In summary, in order to prepare *tetra-arm* gels with high mechanical strength, potential candidates should meet the following selection criteria: (1) the combined use of hydrophilic and hydrophobic macromolecules is a promising route to increase mechanical toughness, although optimisation is required to obtain optimal characteristics; (2) both macromolecules should have mutually reactive end-functional groups to ensure efficient cross-linking processes; (3) the employed macromolecules should have the same chain length; (4) the hydrophobic domains can be used for added functionality, including cargo encapsulation and release.

13.6 Sliding-Ring Hydrogels

Aside from creating homogeneous networks, "sliding-ring" (SR) architectures have also been developed to fabricate tough hydrogels. SR networks utilise an innovative cross-linking motif that differs from both conventional physical and chemical cross-links.[4] The theory of SR networks was first put forward by De Gennes in 1999,[78] who hypothesised that networks with enhanced flexibility and swellability could be fabricated, if a slip-link model was applied. This phenomenon could be conceptually achieved if negatively charged chains were mixed with multi-functional cationic metal (M) cross-linkers to generate networks (Figure 13.9).[4] Upon application of stress, the anionic chains could simply slide along the cationic charges without energy expense, so long as the number of interactions between the components remained constant.[78]

[Figure 13.9 near here]

Figure 13.9. Conceptual illustration of sliding-ring networks as put forward by DeGennes using multi-functional cationic linkers and anionic chains. Reprinted from Physica A: Statistical Mechanics and its Applications, 271, P.-G. de Gennes, Sliding Gels, 231-237, Copyright 1999, with permission from Elsevier.

This concept was experimentally demonstrated by Okumura and Ito in 2001[79] using cyclodextrin (CD)-based host-guest chemistry. Briefly, CDs are cyclic oligosaccharides composed of six to eight *D*-glucose units. Owing to their hydrophobic core, they are able to form inclusion complexes with various guest molecules and polymeric chains, including PEG. In this process, α-CDs form inclusion complexes with PEG, where one α-CD moiety complexes with 2 EG repeat units, resulting in the formation of a pseudopolyrotaxane (PPRX) (Figure 13.10). After inclusion complexation, the end-groups of PEG can be end-capped using bulky end-groups, which results in the formation of polyrotaxanes (PRXs) (Figure 13.10). The PRX structure is unique in that the threaded CDs observe both translational and rotational mobility about the PEG chain. Complete PRX disassociation is prevented by the presence of the bulky end-groups.[4]

[Figure 13.10 near here]

Figure 13.10. Graphical illustration of the synthesis of α-CD/PEG-based polyrotaxanes.

Once PRXs are formed, network formation can take place by chemically inter-linking CDs belonging to different PRXs (usually achieved through the primary hydroxyl groups of the CDs). In this step, a wide range of facile chemistries have been adopted, including simple acid chloride chemistry[79] and click chemistry.[80-82] The SR resultant networks are not based on chemical cross-links, nor do they resemble physical networks. Instead, they are topologically

inter-locked by “figure-of-eight” (two chemically interlinked CDs) CD cross-links. Owing to the dynamic ability of the CDs, when tension is exerted on the network, the applied force can be distributed homogeneously across the entire network by the CD movement (Figure 13.11a).[79] This differs from conventional chemical networks, where any tension exerted onto the networks cannot be equalised due to the static nature of the cross-linking points (Figure 13.11b).[79] Due to the network architecture, SR networks generally observe enhanced elasticity and hence show great potential for various biomedical applications, including artificial blood vessels and skin.

[Figure 13.11 near here]

Figure 13.11. Illustration showing (a) sliding-ring and (b) conventional chemical networks before and during tensile deformation. Reproduced/Adapted from Y. Okumura and K. Ito, *Adv. Mater.*, 2001, **13**, 485. (Ref [79]). Reprinted with permission from John Wiley and Sons.

Furthermore, the inclusion of hydrophobic polymers into SR hydrogels has also been explored.[83] This resulted in networks which observe highly elastomeric characteristics, and thus could be used as scratch-resistant coatings. In this process, the hydroxyl groups of hydroxyproplyated PRXs were used to initiate the ROP of caprolactone (CL), leading to the synthesis of PRXs with hydrophobic poly(caprolactone) (PCL) side chains (Figure 13.12a).[83] Subsequently, the PRX derivative could be further cross-linked with hexamethylene diisocyanate (HMDI) to result in semi-transparent films (Figure 13.12a). The mechanical properties of the dried films resulted in a hysteresis of the stress-strain profile, which is typical of other elastomeric materials (Figure 13.12b). Noteworthy, since the publication of this material in 2008,[83] the PRX modified with PCL has been produced industrially and is

commercially available for use as scratch-resistant coatings, vibration-proof and sound-proof insulation materials for speakers and highly abrasive polishing media.[84]

[Figure 13.12 near here]

Figure 13.12. (a) Graphical illustration of the synthesis of polyrotaxane elastomeric graft copolymer films. (b) Tensile stress-strain curve of the films showing hysteresis. The sample was first drawn up to 100% of strain, followed by recovery to zero strain and subsequent second drawing up to fracture. Reproduced/Adapted from Ref. [83] with permission from The Royal Society of Chemistry.

13.7 Tough Nanocomposite Hydrogels

Aside from tailoring network structure by utilising homogeneous macro-cross-linkers and efficient coupling chemistries, modulating network strength and stiffness can also be induced by the incorporation of discrete nanoparticles (Figure 13.1e) or aggregate-like domains, including hydrophobic association *via* self-assembly (Figure 13.1f) and star polymers (Figure 13.1c) into the hydrogel matrix. In fact, the majority of amphiphilic co-networks are indeed "nanocomposite" (*i.e.*, hydrophobic domains tend to aggregate), while some networks include discrete particle entities to further enhance the mechanical properties (Figure 13.13). In the former case, amphiphilic nanoparticle incorporated networks include networks where either the matrix or the particle themselves are amphiphilic, or the matrix and particle share different polarities.

[Figure 13.13 near here]

Figure 13.13. Graphical illustration of the two most common methods used to fabricate nanocomposite amphiphilic hydrogels.

13.7.1 Clay Nanoparticle Hydrogel Networks

Being readily available, inexpensive and environmentally friendly, clay is one of the most popular materials used as nanoparticles for the modulation of the mechanical strength within hydrogel networks.[85] Nanoclays are crystalline silicates made up of layered tetrahedral and octahedral sheets, with sheet structure and layer arrangement defining the type of clay (Figure 13.14). Furthermore, clay minerals can also act as cross-linkers (*e.g.*, when incorporated with various surfactants or surface modified), and possess a high propensity to be dispersed in aqueous media due to their inherent hydrophilic nature.[85, 86] The degree of exfoliation remains one of the most important parameters in nanoclay nanocomposites as exfoliation increases interfacial contact, and thus enhances mechanical performance.[87, 88] Montmorillonite is a particularly popular type of nanoclay with easily modifiable surface chemistry to induce amphiphilic nature for dispersion into elastomers and hard plastics,[89-91] though Laponite ($Na^{+}_{0.7}[(Mg_{5.5}Li_{0.3})Si_8O_{20}(OH)_4]^{-0.7}$) has become increasingly popular for use in more flexible hydrogel networks.[92-94]

[Figure 13.14 near here]

Figure 13.14. Chemical structures of clay and their respective nanosheets.

Schmidt *et. al.* developed hydrogel networks with increased toughness and elongation till breakage by incorporating Laponite (LP), with an average diameter of 30 nm and a thickness of 1 nm, within an amphiphilic hydrogel network consisting of photocross-linked Pluronic F127 poly(ethylene oxide)-block-poly(propylene oxide)-*block*-poly(ethylene oxide) (PEO-*b*-

PPO-*b*-PEO) diacrylate (Figure 13.15a).[92] Tensile elongation experiments on hydrogel networks with varying LP concentration indicated that increasing the LP concentration led to higher values of the elongation at break and improved tensile strength, while the moduli of the LP hydrogels remained lower than those of hydrogels made solely of Pluronic F127 (Figure 13.15b).[92] These results suggested that both the covalent cross-linking from the polymerised acrylate groups and the physical interactions between LP and Pluronic F127 influence the overall tensile modulus. Interestingly, this trend was in contrast to tetraPEG gels with LP incorporation, where the moduli initially increased with LP concentration but then decreased (LP > 1.6 wt%).[95] Better mechanical performance (*i.e.*, higher elongation at break, toughness and transparency) was seen in this system, and was attributed to the Pluronic facilitating better exfoliation of the LP nanoparticles, whereas the tetraPEG gel system required a specific buffer system. This study suggests that the mechanical properties achieved through clay nanoparticle incorporation are system-specific, and optimal performance depends upon many parameters, among them the polymer chemistry, type of cross-linking, and degree of LP exfoliation.

[Figure 13.15 near here]

Figure 13.15. (a) Schematic representation of the fabrication of clay nanoparticle-embedded hydrogels. (b) Tensile stress-strain curves for various hydrogels. Reprinted (adapted) with permission from C.-J. Wu, A. K. Gaharwar, B. K. Chan and G. Schmidt, Macromolecules, 2011, 44, 8215-8224. Copyright 2011 American Chemical Society.

The compressive properties of LP exfoliated hydrogels have also been studied in a poly(trimethylene carbonate)-*b*-PEG-*b*-poly(trimethylene carbonate) (PTMC-*b*-PEG-*b*-PTMC) polymer system.[86] As the mechanical testing performed on these gels was compressive, results

obtained are incomparable to the tensile testing of the Pluronic F127 gels.[92] Surprisingly, compressive mechanical testing of the swollen hydrogels revealed that an increase in the hydrophobic length (0 to 5 kg mol^{-1}) led to a decrease in the compression modulus by more than a factor of 2. This was attributed to the micellisation of the block copolymers, where the cross-linkable moieties are hidden in the micellar core and thus lead to a decrease in the cross-linking density. However, an increase in overall toughness was obtained when the PTMC length was increased. This was expectedly due to the PTMC enabling the hydrogel to withstand a higher stress due to energy dissipation from the random coil conformation of the PTMC chains and the controlled water absorption in the hydrogels. Upon increasing the incorporation of LP, the compression modulus of the hydrogels increases, indicating the presence of physical interactions between the LP platelets and the polymer network chains. In this design, competing reactions are speculated due to the interface contact between PEG and the nanoclay competing with the interactions between the PTMC blocks.[86]

13.7.2 Nanocomposite Hydrogel Networks via Hydrophobic Association

Although the incorporation of hydrophobic components into hydrophilic networks has been widely used to enhance the mechanical properties, studies which investigate how and where these domains are to be inserted, have not been widely performed. Of particular interest, Qiao and co-workers recently explored how the insertion of stiff hydrophobic aggregates and flexible hydrophobic chains affect overall mechanical performance.[96] These authors demonstrated the importance of this small scale architecture using the PCL-*b*-PEG-*b*-PCL triblock copolymer, and poly([4,4'-bioxepane]-7.7'-dione) (BOD) as the cross-linker, where the former is used as the linear hydrophobic PCL-bearing component, and the latter as the

aggregated hydrophobic domains. Due to the nature of the components, the architecture of the resultant hydrogels is fixed, where the triblock copolymers are connected *via* the terminal hydroxyl groups through BOD cross-linking (Figure 13.16a).[96] To investigate if the precise arrangement of the components affects the mechanical properties, control networks were also synthesised with PEG, PCL and BOD individually incorporated (Figure 13.16b).[96] The compressive mechanical properties of the swollen hydrogels were investigated, revealing that the arrangement of the hydrophobic components within the triblock copolymers significantly increases the overall fracture stress (31.4 MPa), fracture strain (90%), and toughness. Conversely, the randomly distributed control sample exhibited overall compressive fracture stress and fracture strain of around 2-4 MPa and 40-85%, respectively. This significant difference in mechanical properties between the triblock and randomly distributed gels is attributed to the randomly distributed gels displaying a more inhomogeneous distribution of polymer types, thereby reducing their capability to distribute stress evenly.[96] Overall, this shows the mechanical advantage of systematically ordering the aggregated and linear hydrophobic domains instead of allowing them to be randomly organised, and thus defining the nano-architecture of the network.

[Figure 13.16 near here]

Figure 13.16. Graphical illustration comparing the network architectural difference between precisely and randomly incorporating hydrophobic components into a hydrogel network. Reproduced/Adapted from Ref. [96] with permission from The Royal Society of Chemistry.

13.7.3 Tough Hydrogels Containing Self-assembled Micelles

Self-assembled structures, including micelles, are formed from amphiphilic block copolymers. These formed structures can also be incorporated into hydrogel networks to affect the overall mechanical properties. Although not often used to adjust mechanical properties specifically, micelles have been commonly used to induce functionality or act as a multi-functional cross-linker. Unlike the nanoclay-containing networks, micelle-containing networks have a characteristically high fracture strain. As with the nanoclay implementation, tensile stiffness and strength increase, while fracture strain decreases.

Micelles can also make up the entire network and form a structure called a micellar hydrogel. For example, amphiphilic, elastin-like polypeptides (ELP) synthesised by genetically modified *E. coli* can be used to form micelles above 41 °C. Through the hydrophilic terminus of the ELP, network formation can then be achieved through metal (Zn^{2+}) ion co-ordination.[97] The hydrogels exhibit a hierarchical structure which is stable at room temperature, and show a storage modulus of *ca.* 1 MPa.[97] Others have formed physically entangled hydrogels by introducing poly(acrylic acid) (PAA) grafts onto the arms of micelles.[98] Under compressive testing, both the ELP and PAA-micelle hydrogels displayed an increase in compressive stiffness before failure. This is likely due to the hydrophilic block being compressed before the micelles fail after sufficient stress. [97, 98]

As both micelles and hydrogels can act individually as drug delivery systems, micelle/hydrogel nanocomposites have also been employed as delivery systems capable of simultaneously releasing drugs at tuneable rates. [99, 100]

13.7.4 Star Polymer Hydrogel Networks

Star polymers containing both hydrophilic and hydrophobic domains have been used to prepare amphiphilic hydrogels displaying nanophase separation and robust mechanical properties.[64-66, 101-103] The formation of hydrophobic domains within hydrogel networks gives rise to interesting properties and forms the foundation for potential applications in diverse fields such as antifouling, drug delivery, contact lenses, and solid electrolytes. Star polymers are usually more compact and of a higher molecular weight than their conventional linear polymer analogues. This is expected to result in hydrogel networks with fewer defects resulting from chain entanglements and a more regular organisation of the phase separated domains.[101]

Recently, amphiphilic star polymer-based hydrogels were prepared from methyl methacrylate (MMA) and DMAEMA and reported to exhibit phase separated hydrophobic domains.[101] Small-angle neutron scattering (SANS) indicated internal self-assembly and nanophase separation with long-range ordering. The hydrophobic domains were calculated to be between 4-6 nm in size and composed of smaller 1.2-1.6 nm sized sub-domains. Owing to the tertiary amine group of DMAEMA, the hydrogels displayed pH-responsive swelling.

13.8 Conclusion

Over the past few decades a wide array of different methodologies have been developed to overcome the inherent mechanical weakness of conventional polymeric hydrogels synthesised by free radical polymerisation. Issues inherent with conventional systems, include heterogeneous cross-linking density, irregular distribution between cross-link points, and the presence of dangling, non-load bearing chains. In this review Chapter, new methods developed to overcome these disadvantages are presented in detail. Broadly, these approaches can be divided into two categories; (i) altering the network architecture and/or (ii) employing facile

coupling chemistries. In the former category, tough ideal tetraPEG networks have been fabricated by employing macro-monomers of identical size and shape. This gives rise to identical distances between cross-link points and a homogeneous cross-linking density. The use of interpenetrating networks (IPN) and double networks (DN) has also been employed to fabricate tough hydrogels, where one network serves as a sacrificial network. The use of novel architectures including figure-of-eight topological networks has also been explored to create mechanically tough networks. In the latter category, facile, orthogonal coupling chemistries to facilitate hydrogel network formation are also explored. In particular, the wide range of click chemistries is described, along with the benefits these chemistries endow their hydrogel materials with. In this Chapter, special attention towards amphiphilic polymeric co-networks, *i.e.*, networks containing both hydrophilic and hydrophobic domains, is paid. The ability to generate such ideally-structured networks, with improved mechanical and stimuli-responsive properties would allow these polymeric co-networks to be used in a wider range of advanced applications, including soft robotics, biomaterials and materials science.

Acknowledgements

The authors acknowledge the Australian Research Council under the Future Fellowship (FT110100411, G.G.Q.) scheme for financial support of this work. N.C. also acknowledges the Australian Postgraduate Award (APA).

References

1. A. S. Hoffman, *Adv. Drug Delivery Rev.,* 2002, **54**, 3.
2. J. Kopeček, *Nature*, 2002, **417**, 388.
3. O. Wichterle and D. Lím, *Nature*, 1960, **185**, 117.
4. S. Tan, K. Ladewig, Q. Fu, A. Blencowe and G. G. Qiao, *Macromol. Rapid Commun.*, 2014, **35**, 1166.
5. Z. Liu and P. Calvert, *Adv. Mater.*, 2000, **12**, 288.
6. E. Palleau, D. Morales, M. D. Dickey and O. D. Velev, *Nat. Commun.*, 2013, **4**, 2257.
7. K. Wang, X. Zhang, C. Li, H. Zhang, X. Sun, N. Xu and Y. Ma, *J. Mater. Chem. A*, 2014, **2**, 19726.
8. Y. Xu, Z. Lin, X. Huang, Y. Liu, Y. Huang and X. Duan, *ACS Nano*, 2013, **7**, 4042.
9. J. L. Drury and D. J. Mooney, *Biomaterials*, 2003, **24**, 4337.
10. S. Van Vlierberghe, P. Dubruel and E. Schacht, *Biomacromolecules*, 2011, **12**, 1387.
11. J. Li and D. J. Mooney, *Nat. Rev. Mater.*, 2016, **1**, 16071.
12. E. R. Wright, R. A. McMillan, A. Cooper, R. P. Apkarian and V. P. Conticello, *Adv. Funct. Mater.*, 2002, **12**, 149.
13. X. Liu, T.-C. Tang, E. Tham, H. Yuk, S. Lin, T. K. Lu and X. Zhao, *PNAS.*, 2017, **114**, 2200.
14. K. Tian, J. Bae, S. E. Bakarich, C. Yang, R. D. Gately, G. M. Spinks, M. in het Panhuis, Z. Suo and J. J. Vlassak, *Adv. Mater.*, 2017, **29**, 1604827.
15. G. Jing, L. Wang, H. Yu, W. A. Amer and L. Zhang, *Colloids Surf. A.*, 2013, **416**, 86.
16. O. Ozay, S. Ekici, Y. Baran, N. Aktas and N. Sahiner, *Water Research*, 2009, **43**, 4403-4411.
17. A. B. Imran, T. Seki and Y. Takeoka, *Polym. J.*, 2010, **42**, 839.

18. J. Bastide and L. Leibler, *Macromolecules*, 1988, **21**, 2647.

19. T. Tanaka and D. J. Fillmore, *J. Chem. Phys.*, 1979, **70**, 1214.

20. J. P. Gong, *Science*, 2014, **344**, 161.

21. E. Ducrot, Y. Chen, M. Bulters, R. P. Sijbesma and C. Creton, *Science*, 2014, **344**, 186.

22. C. Creton, *Macromolecules*, 2017, **50**, 8297.

23. C. S. Patrickios and T. K. Georgiou, *Curr. Opin. Colloid Interface Sci.*, 2003, **8**, 76.

24. M. Rikkou-Kalourkoti, C. S. Patrickios and T. K. Georgiou, *Model Networks and Functional Conetworks*, In: K. Matyjaszewski and M. Möller M (eds.), *Polymer Science: A Comprehensive Reference*, 2012, Vol 6, pp. 293–308. Amsterdam: Elsevier BV.

25. K. Y. Lee and D. J. Mooney, *Chem. Rev.*, 2001, **101**, 1869.

26. B. Ozcelik, K. D. Brown, A. Blencowe, K. Ladewig, G. W. Stevens, J.-P. Y. Scheerlinck, K. Abberton, M. Daniell and G. G. Qiao, *Adv. Healthcare Mater.*, 2014, **3**, 1496.

27. H. C. Kolb, M. G. Finn and K. B. Sharpless, *Angew. Chem. Int. Ed.*, 2001, **40**, 2004.

28. M. Malkoch, R. Vestberg, N. Gupta, L. Mespouille, P. Dubois, A. F. Mason, J. L. Hedrick, Q. Liao, C. W. Frank, K. Kingsbury and C. J. Hawker, *Chem. Commun.,* 2006, 2774.

29. K. Li, C. Zhou, S. Liu, F. Yao, G. Fu and L. Xu, *React. Funct. Polym.*, 2017, **117**, 81.

30. Y. Jiang, J. Chen, C. Deng, E. J. Suuronen and Z. Zhong, *Biomaterials*, 2014, **35**, 4969.

31. P. M. Kharkar, M. S. Rehmann, K. M. Skeens, E. Maverakis and A. M. Kloxin, *ACS Biomater. Sci. Eng.*, 2016, **2**, 165.

32. A. B. Lowe, *Polym. Chem.*, 2010, **1**, 17.

33. R. K. Iha, K. L. Wooley, A. M. Nyström, D. J. Burke, M. J. Kade and C. J. Hawker, *Chem. Rev.*, 2009, **109**, 5620.

34. D. A. Ossipov and J. Hilborn, *Macromolecules*, 2006, **39**, 1709.

35. U. M. Krishna, A. W. Martinez, J. M. Caves and E. L. Chaikof, *Acta Biomater.*, 2012, **8**, 988.

36. N. J. Agard, J. A. Prescher and C. R. Bertozzi, *J. Am. Chem. Soc.*, 2004, **126**, 15046.

37. C. Ornelas, J. Broichhagen and M. Weck, *J. Am. Chem. Soc.*, 2010, **132**, 3923.

38. N. J. Agard, J. M. Baskin, J. A. Prescher, A. Lo and C. R. Bertozzi, *ACS Chem. Biol.*, 2006, **1**, 644.

39. S. Fu, H. Dong, X. Deng, R. Zhuo and Z. Zhong, *Carbohydr. Polym.*, 2017, **169**, 332.

40. X. Su, L. Bu, H. Dong, S. Fu, R. Zhuo and Z. Zhong, *RSC Advances*, 2016, **6**, 2904.

41. H. Jiang, S. Qin, H. Dong, Q. Lei, X. Su, R. Zhuo and Z. Zhong, *Soft Matter*, 2015, **11**, 6029.

42. J. Xu, T. M. Filion, F. Prifti and J. Song, *Chem. Asian J.*, 2011, **6**, 2730.

43. S. M. Hodgson, E. Bakaic, S. A. Stewart, T. Hoare and A. Adronov, *Biomacromolecules*, 2016, **17**, 1093.

44. J. Zheng, L. A. Smith Callahan, J. Hao, K. Guo, C. Wesdemiotis, R. A. Weiss and M. L. Becker, *ACS Macro Lett.*, 2012, **1**, 1071.

45. C. A. DeForest and K. S. Anseth, *Nat. Chem.*, 2011, **3**, 925.

46. R. J. Ono, A. L. Z. Lee, Z. X. Voo, S. Venkataraman, B. W. Koh, Y. Y. Yang and J. L. Hedrick, *Biomacromolecules*, 2017, **18**, 2277.

47. S. Ishii, H. Kokubo, K. Hashimoto, S. Imaizumi and M. Watanabe, *Macromolecules*, 2017, **50**, 2906.

48. P. M. Imbesi, C. Fidge, J. E. Raymond, S. I. Cauët and K. L. Wooley, *ACS Macro Lett.*, 2012, **1**, 473.

49. L. H. Sperling, *J. Macromol. Sci. Polymer Rev.*, 1977, **12**, 141.

50. L. H. Sperling and V. Mishra, *Polym. Adv. Technol.*, 1996, **7**, 197.

51. J. P. Gong, Y. Katsuyama, T. Kurokawa and Y. Osada, *Adv. Mater.,* 2003, **15**, 1155.

52. S. Naficy, J. M. Razal, P. G. Whitten, G. G. Wallace and G. M. Spinks, *J. Polym. Sci., Part B: Polym. Phys.*, 2012, **50**, 423.

53. Y. Zhao, J. Kang and T. Tan, *Polymer*, 2006, **47**, 7702.

54. L. F. Gudeman and N. A. Peppas, *J. Membr. Sci.*, 1995, **107**, 239.

55. D. J. Waters, K. Engberg, R. Parke-Houben, C. N. Ta, A. J. Jackson, M. F. Toney and C. W. Frank, *Macromolecules*, 2011, **44**, 5776.

56. N. Yuan, L. Xu, H. Wang, Y. Fu, Z. Zhang, L. Liu, C. Wang, J. Zhao and J. Rong, *ACS Appl. Mater. Interfaces*, 2016, **8**, 34034.

57. Y. Bu, H. Shen, F. Yang, Y. Yang, X. Wang and D. Wu, *ACS Appl. Mater. Interfaces*, 2017, **9**, 2205.

58. H. Jia, Z. Huang, Z. Fei, P. J. Dyson, Z. Zheng and X. Wang, ACS Appl. Mater. Interfaces, 2016, **8**, 31339.

59. T. Ube, K. Minagawa and T. Ikeda, *Soft Matter*, 2017, **13**, 5820.

60. J. Li, Z. Suo and J. J. Vlassak, *J. Mater. Chem. B*, 2014, **2**, 6708.

61. J. Chen, Y. Ao, T. Lin, X. Yang, J. Peng, W. Huang, J. Li and M. Zhai, *Polymer*, 2016, **87**, 73.

62. H. J. Zhang, T. L. Sun, A. K. Zhang, Y. Ikura, T. Nakajima, T. Nonoyama, T. Kurokawa, O. Ito, H. Ishitobi and J. P. Gong, *Adv. Mater.*, 2016, **28**, 4884.

63. S. Liu, M. Dong, Z. Zhang and G. Fu, *Polym. Adv. Technol.*, 2017, **28**, 1065.

64. E. N. Kitiri, C. S. Patrickios, C. Voutouri, T. Stylianopoulos, I. Hoffmann, R. Schweins and M. Gradzielski, *Polym. Chem.*, 2017, **8**, 245.

65. M. Rikkou-Kalourkoti, E. N. Kitiri, C. S. Patrickios, E. Leontidis, M. Constantinou, G. Constantinides, X. Zhang and C. M. Papadakis, *Macromolecules*, 2016, **49**, 1731.

66. T. C. Krasia and C. S. Patrickios, *Macromolecules*, 2006, **39**, 2467.

67. T. Matsunaga, T. Sakai, Y. Akagi, U.-i. Chung and M. Shibayama, *Macromolecules*, 2009, **42**, 6245.

68. J. E. Mark and B. Erman, *Rubberlike Elasticity - A Molecular Primer*; Wiley: New York, 1988.

69. T. Sakai, T. Matsunaga, Y. Yamamoto, C. Ito, R. Yoshida, S. Suzuki, N. Sasaki, M. Shibayama and U.-i. Chung, *Macromolecules*, 2008, **41**, 5379.

70. H. Kamata, Y. Akagi, Y. Kayasuga-Kariya, U.-i. Chung and T. Sakai, *Science*, 2014, **343**, 873.

71. K. Nishi, K. Fujii, Y. Katsumoto, T. Sakai and M. Shibayama, *Macromolecules*, 2014, **47**, 3274.

72. H. Kamata, U. Chung, M. Shibayama and T. Sakai, *Soft Matter*, 2012, **8**, 6876.

73. K. Hayashi, F. Okamoto, S. Hoshi, T. Katashima, D. C. Zujur, X. Li, M. Shibayama, E. P. Gilbert, U.-i. Chung, S. Ohba, T. Oshika and T. Sakai, *Nat. Biomed. Eng.*, 2017, **1**, 0044.

74. T. Sakai, Y. Akagi, S. Kondo and U. Chung, *Soft Matter*, 2014, **10**, 6658.

75. S. Czarnecki, T. Rossow and S. Seiffert, *Polymers*, 2016, **8**, 82.

76. X. Ma, R. Usui, Y. Kitazawa, H. Kokubo and M. Watanabe, *Polymer*, 2015, **78**, 42.

77. K. Oshima and Y. Mitsukami, *Polymer*, 2016, **100**, 134.

78. P.-G. de Gennes, *Physica A*, 1999, **271**, 231.

79. Y. Okumura and K. Ito, *Adv. Mater.*, 2001, **13**, 485.

80. S. Tan, A. Blencowe, K. Ladewig and G. G. Qiao, *Soft Matter*, 2013, **9**, 5239.

81. T. Murakami, B. V. K. J. Schmidt, H. R. Brown and C. J. Hawker, *Macromolecules*, 2015, **48**, 7774.

82. J. Wu, H. He and C. Gao, *Macromolecules*, 2010, **43**, 2252.

83. J. Araki, T. Kataoka and K. Ito, *Soft Matter*, 2008, **4**, 245.

84. Y. Noda, Y. Hayashi and K. Ito, *J. Appl. Polym. Sci.*, 2014, **131**, 40509.

85. M. S. Nazir, M. H. Mohamad Kassim, L. Mohapatra, M. A. Gilani, M. R. Raza and K. Majeed, in *Nanoclay Reinforced Polymer Composites: Nanocomposites and Bionanocomposites*, eds. M. Jawaid, A. e. K. Qaiss and R. Bouhfid, Springer Singapore, Singapore, 2016, pp. 35-55.

86. S. Sharifi, S. B. G. Blanquer, T. G. van Kooten and D. W. Grijpma, *Acta Biomaterialia*, 2012, **8**, 4233.

87. P. C. LeBaron, Z. Wang and T. J. Pinnavaia, *Appl. Clay Sci.*, 1999, **15**, 11.

88. F. Kádár, L. Százdi, E. Fekete and B. Pukánszky, *Langmuir*, 2006, **22**, 7848.

89. E. Sancaktar and J. Kuznicki, *Int. J. Adhes. Adhes.*, 2011, **31**, 286.

90. C. R. Silva, R. M. Lago, H. S. Veloso and P. S. Patricio, *J. Braz. Chem. Soc.*, 2018, **29**, 278.

91. H. A. Essawy, M. E. Tawfik, A. M. Khalil and S. H. El-Sabbagh, *Polym. Eng. Sci.*, 2014, **54**, 942.

92. C.-J. Wu, A. K. Gaharwar, B. K. Chan and G. Schmidt, *Macromolecules*, 2011, **44**, 8215.

93. V. I. Paz Zanini, M. Gavilán, B. A. López de Mishima, D. M. Martino and C. D. Borsarelli, *Talanta*, 2016, **150**, 646.

94. A. K. Gaharwar, C. P. Rivera, C.-J. Wu and G. Schmidt, *Acta Biomater.*, 2011, **7**, 4139.

95. M. Fukasawa, T. Sakai, U.-i. Chung and K. Haraguchi, *Macromolecules*, 2010, **43**, 4370.

96. D. Gu, S. Tan, C. Xu, A. J. O'Connor and G. G. Qiao, *Chem. Commun.*, 2017, **53**, 6756.

97. A. Ghoorchian, J. R. Simon, B. Bharti, W. Han, X. Zhao, A. Chilkoti and G. P. López, *Adv. Funct. Mater.*, 2015, **25**, 3122.

98. C. He, K. Jiao, X. Zhang, M. Xiang, Z. Li and H. Wang, *Soft Matter*, 2011, **7**, 2943.

99. T. S. Anirudhan, J. Parvathy and A. S. Nair, *Carbohydrate Polymers*, 2016, **136**, 1118.

100. L. Wei, C. Cai, J. Lin and T. Chen, *Biomaterials*, 2009, **30**, 2606.

101. E. J. Kepola, K. Kyriacou, C. S. Patrickios, M. Simon, M. Gradzielski, M. Kushnir and C. Wesdemiotis, *Macromol. Symp.*, 2017, **372**, 69.

102. E. J. Kepola, E. Loizou, C. S. Patrickios, E. Leontidis, C. Voutouri, T. Stylianopoulos, R. Schweins, M. Gradzielski, C. Krumm, J. C. Tiller, M. Kushnir and C. Wesdemiotis, *ACS Macro Lett.*, 2015, **4**, 1163.

103. S.-i. Yusa, K. Fukuda, T. Yamamoto, K. Ishihara and Y. Morishima, *Biomacromolecules*, 2005, **6**, 663.

Figure Captions

Figure 13.1. Graphical illustration of the new approaches used to fabricate tough polymeric hydrogel networks.

Figure 13.2. Preparation of hydrogels using highly efficient click chemistry. Common click reactions, for example the CuAAC, Diels-Alder, and thiol-ene reactions are shown as well as some of the advantages of click hydrogels over conventional free radical or photo-chemically cross-linked hydrogels.

Figure 13.3. Graphical illustration of ultra-tough DN hydrogels through the sequential photopolymerisation of AMPS followed by AAm. (b) Photograph of the formed DN hydrogels demonstrating resistance to slicing. (c) Compressive stress-strain curve of the DN hydrogel versus the individual singular networks composed of PAMPS and PAAm. Reproduced/Adapted from J. P. Gong, Y. Katsuyama, T. Kurokawa and Y. Osada, *Adv. Mater*., 2003, **15**, 1155. (Ref [51]). Reprinted with permission from John Wiley and Sons.

Figure 13.4. (a) Graphical illustration of the DN hydrogels prepared through the hydrophobic association of the PBMA-*b*-PMAA-*b*-PBMA amphiphilic triblock copolymer, and subsequent hydrogen bonding between the carboxylic acid groups of the first physical network and the amide groups of the second network. (b) Tensile stress-strain curves for the prepared DN and SN hydrogels. (c-d) Photographic images of the DN hydrogels demonstrating high strength and toughness. (e) Cyclic tensile loading-unloading tests of DN networks using different waiting times. (f) Self-recovery properties of DN hydrogels, and (g) Tensile stress-strain curve of the pristine (virgin) DN gel and the healed sample. Reproduced/Adapted from H. J. Zhang, T. L. Sun, A. K. Zhang, Y. Ikura, T. Nakajima, T. Nonoyama, T. Kurokawa, O. Ito, H. Ishitobi and

J. P. Gong, *Adv. Mater.*, 2016, **28**, 4884. (Ref [62]). Reprinted with permission from John Wiley and Sons.

Figure 13.5. Graphical illustration of the synthesis of amphiphilic polymer co-networks, which would subsequently constitute the first network within the final double-network.

Figure 13.6. Graphical illustration depicting the molecular architecture of the ultra-tough tetra-arm gels fabricated from a tetra-arm PEG derivatives.

Figure 13.7. Proposed *tetra-arm* polymer network composed of: (a) same size, tetra-arm hydrophobic (red) and hydrophilic (blue) star homopolymers with reactive end-functional groups; and (b) same size, tetra-arm amphiphilic star block copolymers with reactive end-functional groups.

Figure 13.8. (a) Schematic illustration of the hydrogel components and graphical illustration of the network architecture with varying the thermo-responsive segment fraction *r*. (b) Photographs of the hydrogels exhibiting different swelling ratios, *Q*, in the as-prepared and equilibrium states. (c) Mechanical properties as revealed in the stress-elongation curves of hydrogels equilibrated in PBS at 37 °C. The curves are coloured according to the thermo-responsive segment fraction, *r*. (d) Photographs of hydrogels (r = 0.0 and 0.4) during the elongation tests. From H. Kamata, Y. Akagi, Y. Kayasuga-Kariya, U.-i. Chung and T. Sakai, Science, 2014, 343, 873-875. Reprinted with permission from AAAS.

Figure 13.9. Conceptual illustration of sliding-ring networks as put forward by DeGennes using multi-functional cationic linkers and anionic chains. Reprinted from Physica A: Statistical Mechanics and its Applications, 271, P.-G. de Gennes, Sliding Gels, 231-237, Copyright 1999, with permission from Elsevier.

Figure 13.10. Graphical illustration of the synthesis of α-CD/PEG-based polyrotaxanes.

Figure 13.11. Illustration showing (a) sliding-ring and (b) conventional chemical networks before and during tensile deformation. Reproduced/Adapted from Y. Okumura and K. Ito, *Adv. Mater.*, 2001, **13**, 485. (Ref [79]). Reprinted with permission from John Wiley and Sons.

Figure 13.12. (a) Graphical illustration of the synthesis of polyrotaxane elastomeric graft copolymer films. (b) Tensile stress-strain curve of the films showing hysteresis. The sample was first drawn up to 100% of strain, followed by recovery to zero strain and subsequent second drawing up to fracture. Reproduced/Adapted from Ref. [83] with permission from The Royal Society of Chemistry.

Figure 13.13. Graphical illustration of the two most common methods used to fabricate nanocomposite amphiphilic hydrogels.

Figure 13.14. Chemical structures of clay and their respective nanosheets.

Figure 13.15. (a) Schematic representation of the fabrication of clay nanoparticle-embedded hydrogels. (b) Tensile stress-strain curves for various hydrogels. Reprinted (adapted) with permission from C.-J. Wu, A. K. Gaharwar, B. K. Chan and G. Schmidt, Macromolecules, 2011, 44, 8215-8224. Copyright 2011 American Chemical Society.

Figure 13.16. Graphical illustration comparing the network architectural difference between precisely and randomly incorporating hydrophobic components into a hydrogel network. Reproduced/Adapted from Ref. [96] with permission from The Royal Society of Chemistry.